

Synthesis of Highly Stable Surfactant-free Cu₅ Clusters in Water

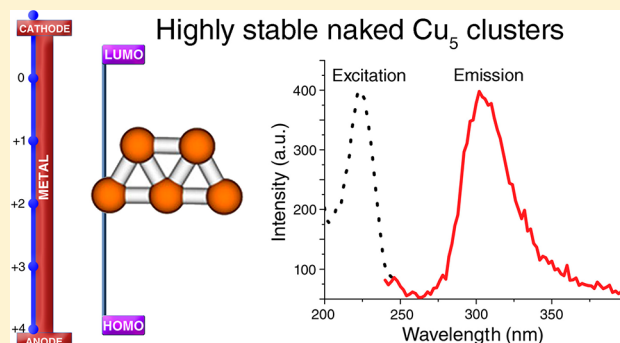
Shahana Huseyinova,[†] José Blanco,[‡] Félix G. Requejo,[§] José M. Ramallo-López,[§] M. Carmen Blanco,[†] David Buceta,^{*,†} and M. Arturo López-Quintela^{*,†}

[†]Physical Chemistry Department, Faculty of Chemistry, and NANOMAG Laboratory, Research Technological Institute, University of Santiago de Compostela, E-15782 Santiago de Compostela, Spain

[‡]INL, International Iberian Nanotechnology Laboratory, 4715-330 Braga, Portugal

[§]Instituto de Investigaciones Físicoquímicas Teóricas y Aplicadas – INIFTA (CONICET, UNLP), 1900 La Plata, Argentina

ABSTRACT: We report the synthesis, for the first time, of small, highly monodisperse Cu₅ clusters in water without any surfactant or protective agent. For this purpose, we used a new approach based on the kinetic control of the reaction, which is achieved with an electrochemical method and using a solution with almost no conductivity (i.e., without added electrolytes commonly used in electrochemical methods). This allows the application of extremely small current densities needed to focus the reaction to synthesize only one selected cluster size. Clusters were characterized by ultraviolet–visible (UV–vis) and fluorescence spectroscopies, atomic force microscopy, electrospray ionization time-of-flight mass spectrometry, X-ray photoelectron spectroscopy, extended X-ray absorption fine structure, and X-ray absorption near-edge spectroscopy, showing the presence of only Cu clusters with five atoms. Contrary to what should be expected, such clusters are very stable and remain unaltered in solution, for at least one year, because of their huge band gap (4.07 eV). Moreover, such Cu₅ clusters are extremely stable to UV irradiation, temperature, and pH.



INTRODUCTION

The discovery of highly efficient and stable catalysts is nowadays one of the most important topics in research because of their importance in industrial processes, affecting not only the economy but also the environment. Nanoparticles have been widely studied in the last decades because of the increase of catalytic efficiency with the surface/volume ratio. However, this increase in efficiency has reached a limit mainly due to two factors: (1) intrinsic limitations of the material because the chemistry of NPs is the same as the bulk and (2) decreasing stability of NPs with decreasing size.^{1,2} These two limitations could be overcome by using subnanometric clusters, also called atomic quantum clusters (AQC). On one hand, clusters seem to display stabilities that are greater than those of nanoparticles, as can be deduced by the fact that nanoparticles are etched in the presence of strong binding ligands to produce stable clusters.³ On the other hand, clusters display a chemistry (highly dependent on cluster size) that is different than that of bulk or nanomaterials due to their different geometrical and electronic structure.^{1,2} Indeed, in recent years many examples of metal clusters being much more efficient catalysts than nanoparticles for different types of chemical reactions have been reported.^{2,4} Some representative examples are, for instance, Ag₃ clusters for the propylene epoxidation by molecular oxygen,⁵ two-dimensional (2D) Au clusters for CO oxidation,⁶ Au clusters for aerobic oxidation of thiols reaching enzymatic activities,⁷ and Pt clusters for the oxygen reduction

reaction.⁸ Although less studied, recently Cu clusters have also been found to be the active species in some Cu-catalyzed reactions, such as selective hydrogenations⁹ and methylene blue reduction.¹⁰

It is interesting to note that, in general, a particular window of cluster sizes has been found to be the active species for a particular reaction^{4,11–14} because of the strong dependence of the geometric and electronic structure on cluster size.

One of the main drawbacks for the use of clusters in catalysis is the availability of simple synthetic protocols for producing monodisperse clusters without using strong binding ligands, which will negatively affect the catalytic properties by not only blocking the adsorption of reactants but also altering the cluster electronic structure.^{1,2,15} Therefore, the development of synthetic protocols to produce clusters without strong binding ligands is a very important matter in catalysis. At the same time, such achievement could provide new insights into the stability of clusters without strong ligands, which is a very controversial matter.

We report here the electrochemical synthesis, for the first time, of small, highly monodisperse Cu₅ clusters in water without any surfactant or protective agent. In recent years,

Special Issue: Kohei Uosaki Festschrift

Received: December 14, 2015

Revised: January 14, 2016

Published: January 20, 2016

copper clusters have been successfully synthesized by other methods with different surfactants.^{16–18} Previously we have shown the electrochemical synthesis of Cu clusters of different sizes using tetrabutyl ammonium (TBA) as protecting agent.¹⁹ In the present work we propose a new approach to produce naked clusters based on the kinetic control of the reaction.²⁰ This is achieved by using a solution with almost no conductivity (i.e., Milli-Q water with no added electrolytes), which allows applying extremely small current densities. Contrary to what should be expected, such clusters are very stable and remain unaltered in solution because of their huge band gap. Moreover, such Cu₅ clusters are extremely stable to ultraviolet (UV) irradiation, temperature, and pH.

MATERIALS AND METHODS

Materials. Copper sheet (99%) and platinum sheet (99.95%) were purchased from Goodfellow. Alumina nanoparticles (average size, ≈ 50 nm) and cloth pads were purchased from Buehler. Sand paper (600 grit) was supplied by Wolfcraft. All water solutions were prepared with Milli-Q grade water using a Direct-Q8UV system from Millipore. MeOH, NaOH, HClO₄, and H₂SO₄ were purchased from Sigma-Aldrich.

CuAQC Synthesis. Copper clusters were obtained by using an electrochemical method with an Autolab PGSTAT 20 potentiostat. A Methrom thermostated-3 electrode electrochemical cell was used, with a copper sheet of 2.5 cm² as working electrode, platinum sheet of 2.5 cm² as counter electrode, and a hydrogen electrode as reference. The working and counter electrodes were placed vertically face to face at a distance of 1 cm. Pure Milli-Q water (conductivity, $\approx 6.26 \mu\Omega/\text{cm}^3$) without any added electrolyte was used, and N₂ was bubbled for 30 min to deaerate the solution. The synthesis was carried out at constant temperature (12 °C) and potential (1 V) during 1000 s under a N₂ atmosphere and strong magnetic stirring. Both the Cu sheet and the Pt sheet were carefully cleaned before synthesis; the copper electrode was polished with sand paper (600 grit) followed by alumina (≈ 50 nm), washed thoroughly with MilliQ water, and sonicated. The platinum electrode was polished only with alumina and then was electrochemically cleaned by cyclic voltammetry in 1 M MeOH/1 M NaOH solution followed by cyclic voltammetry in 1 M H₂SO₄. After the synthesis, the remaining Cu²⁺ ions were precipitated by NaOH and subsequent filtration, and finally the pH was adjusted to 7 by addition of HClO₄. A typical concentration of clusters obtained after purification is in the range 3–5 mg/L. The typical yield of cluster synthesis, taking into account the current–time curve (not shown here) and the Cu content obtained by flame atomic absorption spectroscopy, is around 50%.

CuAQC Characterization. The total Cu content in the cluster samples was analyzed by flame atomic absorption spectroscopy performed with a PerkinElmer 3110 with a Cu hollow cathode lamp of 324.8 nm and a wavelength of 0.5 nm.

Both ultraviolet–visible (UV–vis) and fluorescence spectroscopy were carried out at room temperature using 1 cm path-length Hellma quartz cuvettes. UV–vis spectra were recorded with a Thermo Evolution 300 UV–visible spectrophotometer, and Fluorescence spectra were recorded with a Cary Eclipse Varian fluorimeter.

Atomic force microscopy (AFM) measurements were conducted under normal ambient conditions using an XE-100 instrument (Park Systems) in noncontact mode. The AFM tips were aluminum-coated silicon ACTA from Park Systems with a

resonance frequency of 325 kHz. For AFM imaging, a drop of a diluted sample of CuAQC was deposited onto a freshly cleaved mica sheet (SPI Supplies, grade V-1 Muscovite), which was thoroughly washed with Milli-Q water and dried under nitrogen flow.

Electrospray ionization time-of flight (ESI-TOF) mass spectrometry measurements were performed using a Bruker MicroTOF mass-spectrometer operating in negative ionization mode. Temperature control and nitrogen drying gas (1 $\mu\text{L}/\text{min}$) in ESI source were employed to assist the ionization process. All spectra were acquired in reflectron mode of the TOF mass spectrometer equipped with multistep detection to obtain maximum sensitivity, 15 000 (fwhm); isotopic resolution was observed throughout the entire mass range detected. Spectra were recorded in negative ion mode and averaged from 300 measurements. For full MS scan analysis, the spectra were recorded in the 100 to 1000 m/z range. Calibration was performed employing reserpine (609 m/z) in FIA 10 pg (100:1 S/N 200 $\mu\text{L}/\text{min}$). For the detection of clusters, 10 μL of the CuAQC samples were employed at 0.1 mL/min flow rate in MeOH/H₂O (1:1), using 0.1% formic acid and NaCl (10 mM).

Photoelectron spectra were recorded using a VG Escalab 250iXL spectrometer (VG Scientific) equipped with a hemispherical analyzer and Al KR X-ray monochromated source. An X-ray spot of 500 μm was used to generate photoelectrons, which were collected from a takeoff angle of 90°. The argon partial pressure in the analysis chamber was maintained at 3×10^{-8} mbar during data acquisition by turbomolecular differential pumping. The measurement was done in a constant analyzer energy mode (CAE) with a 100 eV pass energy for survey spectra and 20 eV pass energy for high-resolution spectra. The intensities were estimated by calculating the area under each peak after subtraction of the S-shaped background. Binding energies (BEs) of Cu 2p could be determined by referencing to the adventitious C 1s peak at 285.0 eV. Atomic ratios were computed from peak intensity ratios and Schofield atomic sensitivity factors. Samples for X-ray photoelectron spectroscopy (XPS) analysis were prepared by leaving a drop of solution containing CuAQC in water on a piece of silicon wafer mirror finish polished, quickly evaporating the solvent, and immediately introducing the sample into the XPS prechamber under high-vacuum conditions. Ar⁺ ions (1.5 keV, 60 s) were employed to remove adventitious carbon, which comes from the surface sample exposure to the atmosphere, and to remove also possible oxides at the sample surface. The amount of material removed is a function of the incident energy and sputtering time. Samples were kept rotating to avoid a shadow effect. The efficiency of the sputtering process was checked by the disappearance of the Si oxide native layer from the silicon wafer substrate. Bombardment was performed using an EXOS ion gun incorporated into the equipment, provided with a scanning unit to raster the ion beam, operating at a voltage of 1.5 kV and a scan size of 2 mm, producing a sample current of 0.3 μA during 60 s of bombardment. The higher oxidation state of copper(II) can be identified by a shakeup satellite at ~ 10 eV from the Cu 2p_{3/2} main peak. This satellite peak is not present for other chemical species of copper, such as Cu(0) or Cu(I).

X-ray absorption spectroscopy (XAS) measurements were performed at the XAFS2 beamline of the LNLS (Laboratório Nacional de Luz Síncrotron), Campinas, Brazil. X-ray absorption near-edge spectroscopy (XANES) and extended X-ray absorption fine structure (EXAFS) spectra at the Cu K-

edge (8979 eV) were recorded at room temperature using a Si(111) single channel-cut crystal monochromator. Cu₅ clusters in water solution were placed in a liquid cell with kapton windows, and XAS measurements were performed in fluorescence mode using a 16-element Ge detector. To increase the signal-to-noise ratio, six scans were averaged. Cu references were measured in transmission mode with two ion chambers as detectors. XANES spectra normalization, EXAFS oscillations extraction, and fitting procedure were performed using the "IFEFFIT" software package.²¹

RESULTS AND DISCUSSION

CuAQC's Characterization. Figure 1a shows the UV–vis spectrum of the synthesized clusters, with an absorption band

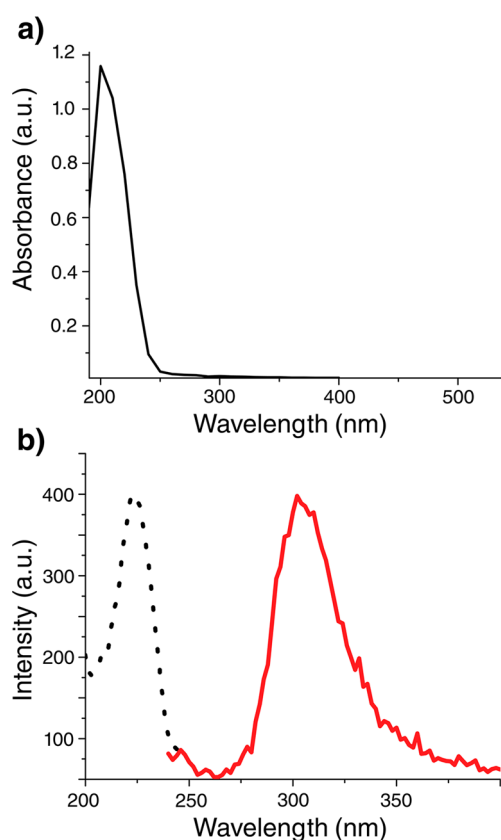


Figure 1. (a) UV–vis spectrum and (b) emission ($\lambda_{\text{exc}} = 224$ nm, red) and excitation ($\lambda_{\text{emi}} = 305$ nm, black) spectra of small Cu clusters in water with no surfactant.

located at ≈ 220 nm, without the presence of the Cu Plasmon band (around 560 nm).²² Although absorption of Cu clusters has been previously reported in the UV range, in the present case the energies are higher, indicating that cluster band gaps are bigger; thus, clusters are smaller.^{19,23–25} In general, clusters are known for their photoluminescent properties,^{19,23,24} with emission wavelengths depending on the cluster size. Figure 1b shows the excitation and emission spectra of the synthesized Cu clusters, with an excitation band at 224 nm and an emission band at 305 nm.

Cluster size can be calculated from spectroscopic data by using the simple spherical Jellium model, following the expression $N = (E_F/E_G)^3$, where N is the number of atoms of the cluster, E_F the Fermi level of the metal, and E_G the band gap.^{26,27} Within this approach, large absorption or emission

energies are associated with large band gaps, which in turn are associated with small cluster sizes. This model has been proven to be a very good approximation, with values comparable to those obtained by density functional theory or experimentally;²⁷ the agreement is much better for naked clusters (or capped with weak bounded ligands) because of the influence of ligands in their electronic and geometric structure.¹⁵ Within this approach the observed emission energy at $\lambda = 305$ nm should correspond to a cluster band gap of 4.07 eV. Using the Jellium model, one can deduce that the obtained clusters should contain only five atoms. Moreover, the observation of a simple band in both UV–vis and fluorescence spectroscopies indicates the high monodispersity of the obtained clusters.

Small clusters have low melting points; therefore, techniques like high-resolution transmission electron microscopy or high-resolution scanning transmission electron microscopy are not very useful to characterize them because of the high-energy electron beam.²⁸ On the other hand AFM, because of its high Z resolution, is a convenient technique for investigating the synthesized CuAQC's because, if they have less than 7 atoms, they should present a 2D geometry.¹⁴ Figure 2 shows AFM images of the synthesized Cu clusters deposited over a mica substrate. AFM results show the presence of CuAQC islands of ≈ 300 pm in height, suggesting a 2D geometry and confirming the presence of clusters with less than 7 atoms, in accordance

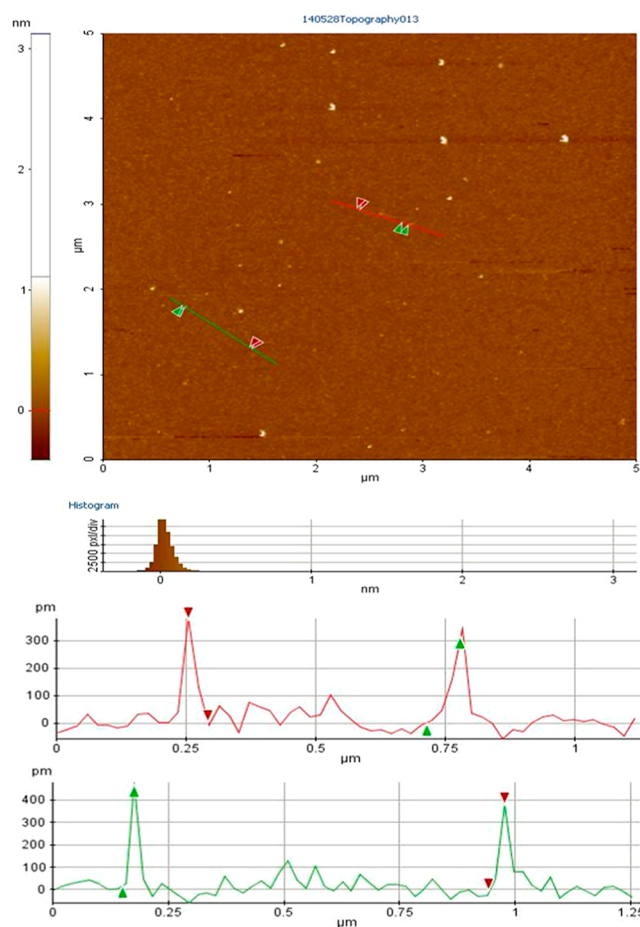


Figure 2. (Top panel) AFM image of CuAQC's deposited on mica (mean square roughness ≈ 150 pm) and (bottom panels) AFM height profiles measured through the red and green lines (plotting distance (x -axis) against height (y -axis)).

with the results deduced above from the UV–vis and luminescence spectroscopies.

To obtain a more precise characterization, ESI-TOF mass spectrometry was carried out, and the results can be seen in Figure 3. Because this technique uses very soft ionization,

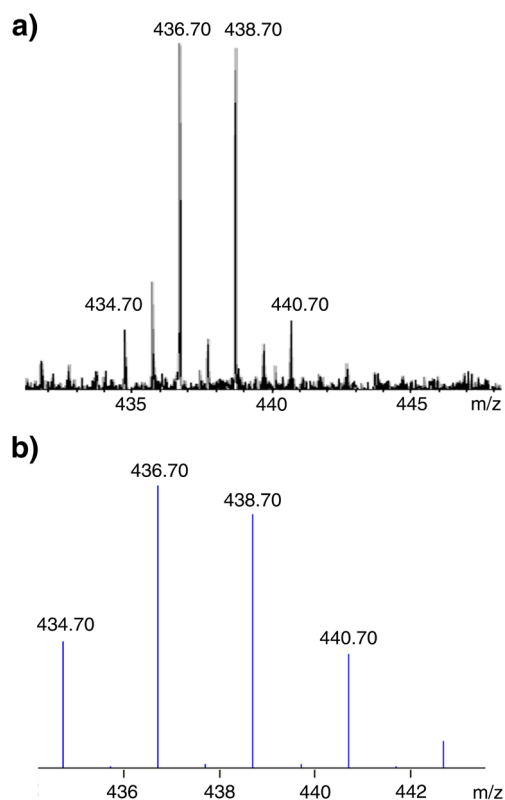
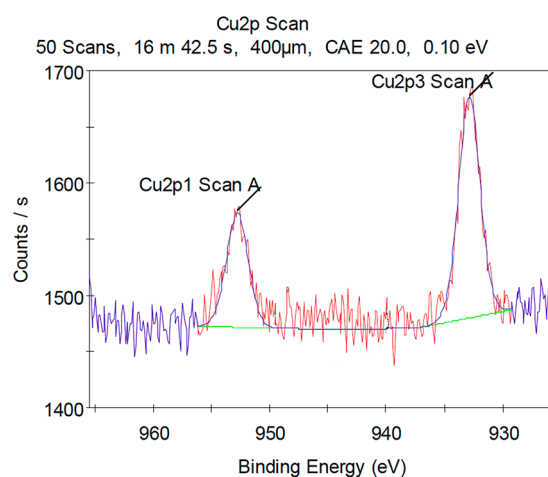


Figure 3. ESI-TOF mass spectrum of CuAQC detected in negative mode at $m/z = 436.70$ $[\text{Cu}_5(\text{OH})_2(\text{H}_2\text{O})\text{HCOONa}]^-$: (a) experimental and (b) theoretical.

fragmentation can be avoided, which is ideal for the characterization of small metal clusters.^{29,30} One main peak at 436.70 was obtained in the negative mode, assigned to $[\text{Cu}_5(\text{OH})_2(\text{H}_2\text{O})\text{HCOONa}]^-$, confirmed by the isotopic distribution of Cu. Mass spectrometry conclusively confirms the previous characterization methods, indicating the presence of only Cu_5 AQC.

Additionally, XPS analysis was performed with the aim of studying the oxidation state of the copper atoms in the synthesized clusters. One can distinguish between zero and higher oxidation states of Cu atoms by a shift in the Cu $2p_{3/2}$ core level peak to higher binding energies and the appearance of shakeup satellite peaks around 945 eV (Cu $2p_{3/2}$) and 965 eV (Cu $2p_{1/2}$).¹⁹ XPS of our CuAQC samples can be seen in Figure 4, showing that Cu $2p_{3/2}$ has a binding energy at 932.86 eV and Cu $2p_{1/2}$ at 952.79 eV, disregarding the presence of Cu(II) in the samples. It can be also seen that no clear satellite peak is observed in the marked region, indicating that clusters are most probably formed by Cu(0); however, due to the poor resolution in the satellite peak area, this aspect needs further clarification. In any case, the obtained results are similar to those previously reported for TBA-stabilized Cu clusters.¹⁹

To examine in more detail the oxidation state of the clusters, XANES spectra were measured for the first time for such small size Cu clusters. Figure 5a shows the XANES spectra at the Cu



Elemental ID and Quantification

Name	Peak BE	FWHM eV	Area (P) CPS.eV	Atomic %	Q
Cu2p3 Scan A	932.86	2.16	460.82	49.45	1
Cu2p1 Scan A	952.79	2.15	238.54	50.55	1

Figure 4. (Top panel) High-resolution XPS spectrum fitted of CuAQC and (bottom panel) Cu 2p elemental ID and quantification.

K-edge of Cu_5 clusters and reference compounds. The analysis of the electronic state of Cu atoms considering the energy of the absorption edge and the shape of the spectra indicate the average oxidation state of Cu atoms in Cu_5 clusters; although the value cannot be exactly established by this technique, it confirms that it could be between Cu^0 and Cu^{1+} . Moreover, structural information can be obtained from the EXAFS spectra. Figure 5b compares the EXAFS oscillations of Cu_5 clusters and Cu foil. Although the cluster signal presents a very weak EXAFS oscillation, it is observed that the main characteristics of the signal of the foil are also present in clusters, indicating that the main contribution to the EXAFS oscillations around the absorbing Cu atom is produced by a shell of Cu atoms at a similar distance to that of the foil. The strong difference in the amplitude between both oscillations is a proof of a big reduction of the coordination number in the Cu_5 clusters. In effect, if we perform a fit of the EXAFS signal proposing a Cu–Cu shell, we obtain a coordination number between 2 and 3, which ideally corresponds to a Cu cluster with less than 10 atoms independent of their geometry.³¹ All these results nicely agree with the above-mentioned results obtained by other techniques.

It is interesting to note that the experimental conditions used in this work for the synthesis of Cu_5 AQC are very similar to those previously used for the synthesis of Ag_3 AQC.³² The small difference in size can be explained by the difference in the reduction potentials of both metals in accordance with the kinetic control model.²⁰

CuAQC Stability. The synthesized Cu clusters were stable while stored at room temperature for at least 2 years, as can be seen in Figure 6a in which no appreciable change in UV–vis or fluorescence spectra is observed. The stability of CuAQC was tested against UV irradiation, temperature, and pH. The results of the stability experiments are shown in Figure 6.

Photobleaching experiments were carried out by irradiating the CuAQC at 220 nm for 24h. Both UV–vis and fluorescence spectra showed no change whatsoever, indicating the good photobleaching resistance of the synthesized clusters.

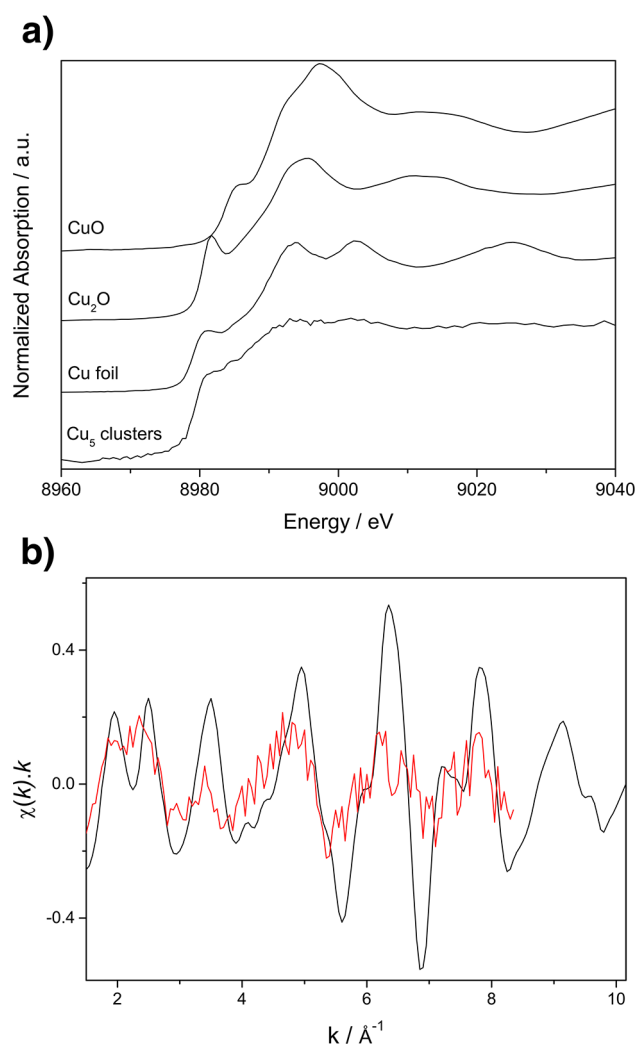


Figure 5. (a) Normalized XANES spectra at the Cu K-edge of Cu_5 clusters and reference compounds and (b) normalized EXAFS spectra (weighted by k to the first power) at the Cu K-edge of the Cu_5 clusters (red line) and reference Cu foil (black line).

To determine the resistance toward temperature of the synthesized CuAQC, one sample was stored at 60 °C for several days. Similar to the photobleaching experiments, neither the UV–vis nor the fluorescence spectrum changed at all after this period.

The last stability test of CuAQC was done against pH. As can be seen in Figure 6d, CuAQC are stable in the whole pH range (1 to 14, achieved by addition of HClO_4 or NaOH). This result is similar to previous experiments carried out with protected Cu clusters,¹⁹ but in this case, the pH range is larger, once again confirming the great stability of the synthesized clusters in comparison to bulk metal or nanoparticles.

Figure 7 shows a scheme of the expected positions of the highest occupied molecular orbital (HOMO) and lowest unoccupied molecular orbital (LUMO) levels for Cu_5 clusters, considering the previous estimation of their band gap (≈ 4.1 eV) and the change in the Fermi level with the cluster size reported before ($E_{\text{F}}(\text{CuAQC}) = -E_{\text{F}}(\text{Cu}_{\text{bulk}}) + N^{-1/3}$). It can be seen that oxidation of clusters can occur only at huge oxidation potentials (greater than ≈ 3.8 V) indicating that clusters can hardly be oxidized. Therefore, the reason for the large stability displayed by the synthesized small Cu_5 clusters is

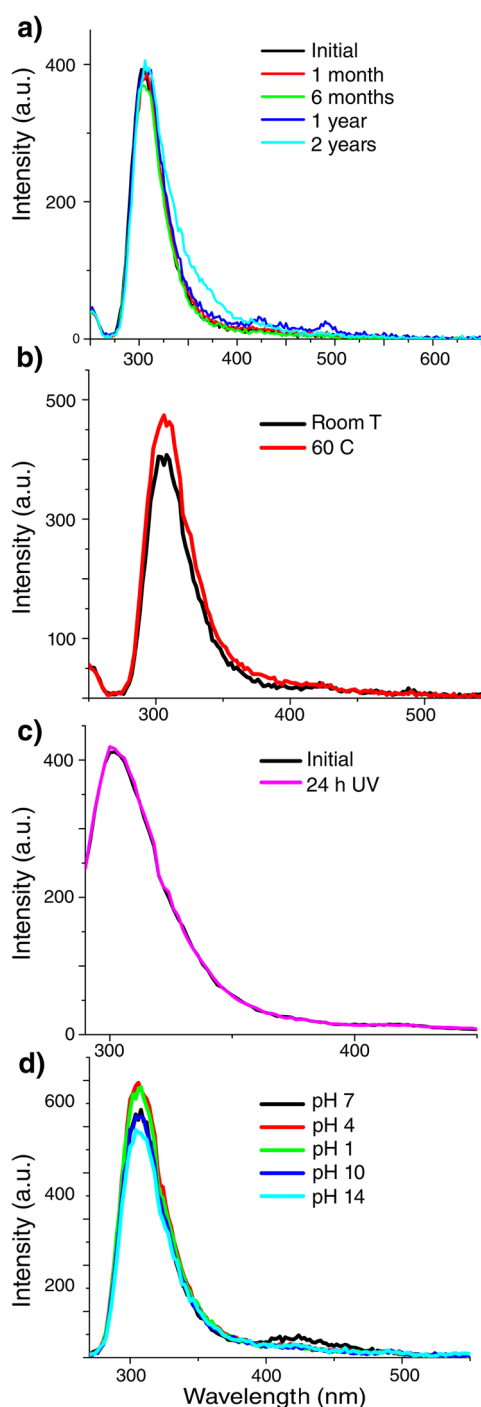


Figure 6. Emission spectra of CuAQC (a) stored at room temperature for two years, (b) heated at 60 °C for 3 days, (c) before and after irradiation at 220 nm for 24 h, and (d) at different pH between 1 and 14.

their huge band gap, which in contrast to larger clusters or small metal particles makes them highly resistant to oxidation.

In the case of metal particles, aggregation is driven by the decrease of the surface energy. Therefore, there is a need to use capping protecting agents, which are more important as the size of the particle is reduced because of the increase of the surface/volume ratio. However, the synthesized 2D- Cu_5 clusters have to break and form new Cu–Cu bonds to aggregate and give 3D- Cu_{10} clusters, which have a completely different geometric and electronic structure.¹⁴ Due to such differences in structure,

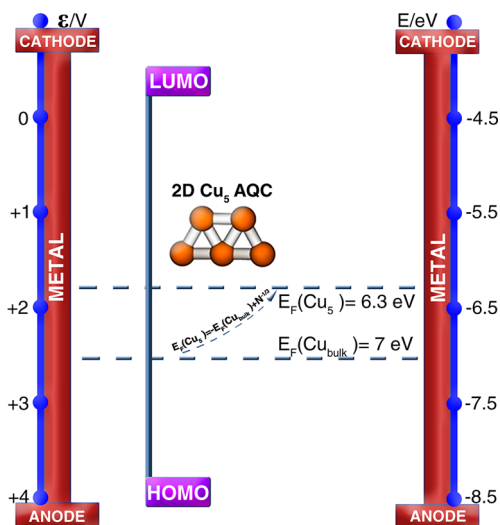


Figure 7. Scheme of the expected positions of the HOMO and LUMO levels for Cu_5 clusters.

contrary to what occurs with metal nanoparticles, the aggregation (fusion) of clusters needs to overcome an energy barrier, similar to any other chemical reaction. The above-mentioned experiments with temperature show that such activation energy for unsupported clusters should be much higher than 2.8 kJmol^{-1} .

In conclusion, we have shown the synthesis of small 2D- Cu_5 clusters without binding ligands, which are very stable because of their high HOMO–LUMO gap (4.07 eV) and are stable for years in water at temperatures up to $60 \text{ }^\circ\text{C}$, under UV irradiation, and even exposed to extreme pH conditions.

AUTHOR INFORMATION

Corresponding Authors

*E-mail: malopez.quintela@usc.es.

*E-mail: buceta.david@gmail.com.

Notes

The authors declare no competing financial interest.

ACKNOWLEDGMENTS

This Project has received funding from the European Union's FP7 FutureNanoNeeds under Grant Agreement 604602; the H2020 INSPIRED research and innovation program under Grant Agreement 646155; and the POCTEP-FEDER programs (InveNNta Project); as well as from the MINECO, Spain (MAT2012-36754-C02-01); Xunta de Galicia, Spain (Grupos Ref. Comp. GRC2013-044, FEDER Funds); and Obra Social Fundación La Caixa, Ref. OSLC-2012-007. F.G.R. and J.R.L. acknowledge the financial support received from UNLP (Argentina, Project 11/X654), CONICET (Argentina, PIP No. 3079), and LNLS (Brasil, Project XAFS1-18861). D.B. acknowledges the postdoc grant from Xunta de Galicia, Spain (POS-A/2013/018).

REFERENCES

- (1) Fuentes, J. C.; Rey, J. R.; Lopez-Quintela, M. A. Synthesis of Subnanometric Metal Nanoparticles. In *Encyclopedia of Nanotechnology*; Bhushan, B., Ed.; Springer Verlag: Dordrecht, The Netherlands, 2012; pp 2639–2648.
- (2) Tyo, E. C.; Vajda, S. Catalysis by Clusters with Precise Numbers of Atoms. *Nat. Nanotechnol.* **2015**, *10* (7), 577–588.

- (3) Muhammed, M. A.; Ramesh, S.; Sinha, S. S.; Pal, S. K.; Pradeep, T. Two Distinct Fluorescent Quantum Clusters of Gold Starting from Metallic Nanoparticles by pH-Dependent Ligand Etching. *Nano Res.* **2008**, *1* (4), 333–340.

- (4) Buceta, D.; Piñeiro, Y.; Vázquez-Vázquez, C.; Rivas, J.; López-Quintela, M. Metallic Clusters: Theoretical Background, Properties and Synthesis in Microemulsions. *Catalysts* **2014**, *4* (4), 356–374.

- (5) Lei, Y.; Mehmood, F.; Lee, S.; Greeley, J.; Lee, B.; Seifert, S.; Winans, R. E.; Elam, J. W.; Meyer, R. J.; Redfern, P. C.; et al. Increased Silver Activity for Direct Propylene Epoxidation via Subnanometer Size Effects. *Science* **2010**, *328* (5975), 224–228.

- (6) Herzing, A. A.; Kiely, C. J.; Carley, A. F.; Landon, P.; Hutchings, G. J. Identification of Active Gold Nanoclusters on Iron Oxide Supports for CO Oxidation. *Science (Washington, DC, U. S.)* **2008**, *321* (5894), 1331–1335.

- (7) Corma, A.; Concepción, P.; Boronat, M.; Sabater, M. J.; Navas, J.; Yacamán, M. J.; Larios, E.; Posadas, A.; López-Quintela, M. A.; Buceta, D.; et al. Exceptional Oxidation Activity with Size-Controlled Supported Gold Clusters of Low Atomicity. *Nat. Chem.* **2013**, *5*, 775–781.

- (8) Yamamoto, K.; Imaoka, T.; Chun, W.-J.; Enoki, O.; Katoh, H.; Takenaga, M.; Sonoi, A. Size-Specific Catalytic Activity of Platinum Clusters Enhances Oxygen Reduction Reactions. *Nat. Chem.* **2009**, *1* (5), 397–402.

- (9) Maity, P.; Yamazoe, S.; Tsukuda, T. Dendrimer-Encapsulated Copper Cluster as a Chemoselective and Regenerable Hydrogenation Catalyst. *ACS Catal.* **2013**, *3* (2), 182–185.

- (10) Vilar-Vidal, N.; Rivas, J.; López-Quintela, M. A. Size Dependent Catalytic Activity of Reusable Subnanometer Copper(0) Clusters. *ACS Catal.* **2012**, *2* (8), 1693–1697.

- (11) Attia, Y. A.; Buceta, D.; Blanco-Varela, C.; Mohamed, M. B.; Barone, G.; López-Quintela, M. A. Structure-Directing and High-Efficiency Photocatalytic Hydrogen Production by Ag Clusters. *J. Am. Chem. Soc.* **2014**, *136* (4), 1182–1185.

- (12) Buceta, D.; Blanco, M. C.; López-Quintela, M. A.; Vukmirovic, M. B. Critical Size Range of Sub-Nanometer Au Clusters for the Catalytic Activity in the Hydrogen Oxidation Reaction. *J. Electrochem. Soc.* **2014**, *161* (7), D3113–D3115.

- (13) Vilar-Vidal, N.; Rey, J. R.; López Quintela, M. A. Green Emitter Copper Clusters as Highly Efficient and Reusable Visible Degradation Photocatalysts. *Small* **2014**, *10*, 3632–3636.

- (14) Fernández, E.; Boronat, M.; Corma, A. Trends in the Reactivity of Molecular O₂ with Copper Clusters: Influence of Size and Shape. *J. Phys. Chem. C* **2015**, *119* (34), 19832–19846.

- (15) Walter, M.; Akola, J.; Lopez-Acevedo, O.; Jadzinsky, P. D.; Calero, G.; Ackerson, C. J.; Whetten, R. L.; Gronbeck, H.; Hakkinen, H. A Unified View of Ligand-Protected Gold Clusters as Superatom Complexes. *Proc. Natl. Acad. Sci. U. S. A.* **2008**, *105* (27), 9157–9162.

- (16) Wei, W.; Lu, Y.; Chen, W.; Chen, S. One-Pot Synthesis, Photoluminescence, and Electrochemical Properties of Subnanometer-Sized Copper Clusters. *J. Am. Chem. Soc.* **2011**, *133* (7), 2060–2063.

- (17) Lu, Y.; Chen, W. Sub-Nanometre Sized Metal Clusters: From Synthetic Challenges to the Unique Property Discoveries. *Chem. Soc. Rev.* **2012**, *41* (9), 3594–3623.

- (18) Gao, X.; Lu, Y.; Liu, M.; He, S.; Chen, W. Sub-Nanometer Sized Cu₆(GSH)₃ Clusters: One-Step Synthesis and Electrochemical Detection of Glucose. *J. Mater. Chem. C* **2015**, *3* (16), 4050–4056.

- (19) Vilar-Vidal, N.; Blanco, M. C.; Lopez-Quintela, M. A.; Rivas, J.; Serra, C. Electrochemical Synthesis of Very Stable Photoluminescent Copper Clusters. *J. Phys. Chem. C* **2010**, *114* (38), 15924–15930.

- (20) Piñeiro, Y.; Buceta, D.; Calvo, J.; Huseynova, S.; Cuerva, M.; Pérez, Á.; Domínguez, B.; López-quintela, M. A. Large Stability and High Catalytic Activities of Sub-Nm Metal (0) Clusters: Implications into the Nucleation and Growth Theory. *J. Colloid Interface Sci.* **2015**, *449*, 279–285.

- (21) Ravel, B.; Newville, M. ATHENA, ARTEMIS, HEPHAESTUS: Data Analysis for X-Ray Absorption Spectroscopy Using IFEFFIT. *J. Synchrotron Radiat.* **2005**, *12* (4), 537–541.

(22) Lisiecki, I.; Pileni, M. P. Copper Metallic Particles Synthesized "in Situ" in Reverse Micelles: Influence of Various Parameters on the Size of the Particles. *J. Phys. Chem.* **1995**, *99* (14), 5077–5082.

(23) Barthel, M. J.; Angeloni, I.; Petrelli, A.; Avellini, T.; Scarpellini, A.; Bertoni, G.; Armirotti, A.; Moreels, I.; Pellegrino, T. Synthesis of Highly Fluorescent Copper Clusters Using Living Polymer Chains as Combined Reducing Agents and Ligands. *ACS Nano* **2015**, *9*, 11886.

(24) Vázquez-Vázquez, C.; Bañobre-López, M.; Mitra, A.; López-Quintela, M. A.; Rivas, J. Synthesis of Small Atomic Copper Clusters in Microemulsions. *Langmuir* **2009**, *25* (14), 8208–8216.

(25) Ziahashabi, A.; Ghodselahe, T.; Heidari saani, M. Localized Surface Plasmon Resonance Properties of Copper Nano-Clusters: A Theoretical Study of Size Dependence. *J. Phys. Chem. Solids* **2013**, *74* (7), 929–933.

(26) Zheng, J.; Nicovich, P. R.; Dickson, R. M. Highly Fluorescent Noble-Metal Quantum Dots. *Annu. Rev. Phys. Chem.* **2007**, *58*, 409–431.

(27) Santiago-González, B.; López-Quintela, M. A. New Strategies and Synthetic Routes to Synthesize Fluorescent Atomic Quantum Clusters. In *Functional Nanometer-Sized Clusters of Transition Metals: Synthesis, Properties and Applications*; Chen, W., Chen, S., Eds.; The Royal Society of Chemistry: Cambridge, 2014; pp 25–50.

(28) Iijima, S.; Ichihashi, T. Structural Instability of Ultrafine Particles of Metals. *Phys. Rev. Lett.* **1986**, *56* (6), 616–619.

(29) Guo, J.; Kumar, S.; Bolan, M.; Desireddy, A.; Bigioni, T. P.; Griffith, W. P. Mass Spectrometric Identification of Silver Nanoparticles: The Case of Ag₃₂(SG)₁₉. *Anal. Chem.* **2012**, *84*, 5304–5308.

(30) González, B. S.; Blanco, M. C.; López-Quintela, M. A. Single Step Electrochemical Synthesis of Hydrophilic/hydrophobic Ag₅ and Ag₆ Blue Luminescent Clusters. *Nanoscale* **2012**, *4*, 7632–7635.

(31) Fritsche, H.-G.; Benfield, R. Exact Analytical Formulae for Mean Coordination Numbers in Clusters. *Z. Phys. D: At., Mol. Clusters* **1993**, *26* (1), 15–17.

(32) Buceta, D.; Busto, N.; Barone, G.; Leal, J. M.; Domínguez, F.; Giovanetti, L. J.; Requejo, F. G.; García, B.; López-Quintela, M. A. Ag₂ and Ag₃ Clusters: Synthesis, Characterization, and Interaction with DNA. *Angew. Chem., Int. Ed.* **2015**, *54* (26), 7612–7616.